that remains operative in the dark and whether these reactions proceed by formation of separate complexes with iron or, alternatively, involve the reorganization of an oxidized nitrogenous intermediate are questions that need to be resolved before the reaction mechanism can be fully elucidated.

Acknowledgment. This study was funded by the Marine Chemistry Program of the National Science Foundation under Grant No. OCE-8409069, for which we are deeply grateful. We also acknowledge support from the Air Resources Laboratory (GMCC) of the National Oceanic and Atmospheric Administration. We thank Dave Carlson and James Krueger for valuable discussions and for reviewing the manuscript.

Registry No. NH_2OH, 7803-49-8; Fe^{3+}, 20074-52-6; N_2O, 10024-97-2.

Contribution from the Section de Biologie, U. 219 INSERM, Bât. 112, Institut Curie, Centre Universitaire, 91405 Orsay Cedex, France

Electron Paramagnetic Resonance Studies of the Intramolecular Coordination in Superstructured Iron(III) Porphyrins

Corinne Schaeffer,* Michel Momenteau, Joël Mispelter, Bernard Loock, Christiane Huel, and Jean-Marc Lhoste

Received February 28, 1986

The electron paramagnetic resonance spectra of iron(III) both face hindered porphyrins (basket-handle porphyrins) in which oxygen or nitrogen ligand donors are incorporated into one of the two handles are reported in the absence or in the presence of exogenous ligands. The ESR spectra of the ferric chloride complexes of compounds α-5,15-[2,2′-(6-hydroxyundecanediamido)diphenyl]-β-10,20-[2,2′-(dodecanediamido)diphenyl]porphyrin ((**11**)Cl), α-5,15-β-10,20-bis[2,2′-(6-hydroxyundecanediamido)diphenyl]-porphyrin ((**13**)Cl), and α-5,15-[2,2′-(6-hydroxyundecanediamido)diphenyl]-β-10,20-[2,2′-(pyridine-3,5-diyldipropionamido)diphenyl]porphyrin ((**14**)Cl) in the presence of tributylamine are characteristic of high-spin five-coordinated complexes with a strong rhombic distortion attributed to the intramolecular coordination of the alkoxo group. A similar spectrum is obtained directly from the compound {α-5,15-[2,2′-(6-oxyundecanediamido)diphenyl]-β-10,20-[2,2′-(3,3′-(*p*-phenylene)dipropionamido)diphenyl]-porphyrin}iron(III) (**12**), which elutes from thin-layer chromatography without exogenous counterion. Addition of sodium alkoxide or 1-methylimidazole to a chloroform solution of these compounds produces low-spin six-coordinated complexes. Their ESR spectra depend not only on the nature of the appended ligand but also on the nature of the starting counterion of iron(III) and on the exogenous ligand type. From the analysis of ESR *g* values, which describes the tetragonal and rhombic distortion of the octahedral ligand field, it was possible to identify the axial ligands in mixed-ligand or bis(ligand) complexes. The formation of the different complexes are discussed with respect to the electronic properties and constraint of the axial ligands.

Introduction

The state and the nature of the heme iron–ligand bonds are closely related to the function of hemoproteins. Thus, imidazole is known to coordinate axially to iron in hemoglobin, myoglobin, cytochromes, and some peroxidases.[1-3] Anionic ligands such as imidazolate,[4] mercaptide,[5] and phenoxide[6] have also been proven as proximal iron ligands in other type of hemoproteins. In particular, the latter ligand may play a determinant role in controlling the catalytic activity of catalase.[7] Such a ligand is also found in several hemoglobin mutants that permanently remain oxidized (Fe(III)) in vivo where the proximal or distal histidines are replaced by tyrosine, in either the α or β chain.[6,8,9] Simulations of the coordination sphere of iron in these hemoproteins have been previously performed by reactions of simple iron porphyrins with free alkoxides and phenoxides.[10-14] Another approach is to use compounds in which the axial ligand is covalently attached to the porphyrin ring. These compounds permit the strict control of the coordination number on the iron and eliminate the need for excess free ligand in solution.[15-18] We have applied with success this concept in the ether- and amide-"basket-handle" porphyrins, both involving a pyridine or imidazole ligand on one side,[19] in order to study the main factors for O_2 and CO binding in hemoglobin and myoglobin.[20]

The present work reports on the ESR study of the interaction of iron(III) amide-basket-handle porphyrins in which alcohol, alkoxide, pyridine, or imidazole are inserted into one or both handles with several neutral or anionic ligands. The results provide new insights into the magnetic properties of alkoxide complexes, which are compared to those of well-established ferric porphyrin derivatives.

Results

Formulas of the functionalized amide-basket-handle porphyrins (a-BHP) we have investigated are shown in Figure 1. They

(1) Antonioni, E.; Brunori, M. *Hemoglobin and Myoglobin in Their Reactions with Ligands*; North-Holland: Amsterdam, 1971.
(2) Margoliash, E. *Heme and Hemoproteins*; Chance, B., Estabrook, R. W., Yonetani, T. Eds.; Academic: London, 1966.
(3) Mathews, F. S.; Levine, M.; Argos, P. *J. Mol. Biol.* **1972**, *64*, 449–464.
(4) Morrison, M.; Schonbaun, G. R. *Annu. Rev. Biochem.* **1976**, *45*, 861–888.
(5) (a) Stern, J. O.; Peisach, J. *J. Biol. Chem.* **1974**, *249*, 7495–7498. (b) Cramer, S. P.; Dawson, J. H.; Hodgson, K. O.; Hager, L. P. *J. Am. Chem. Soc.* **1978**, *100*, 7282–7290.
(6) Greer, J. *J. Mol. Biol.* **1971**, *59*, 107–126.
(7) Reid, T. J., III; Murthy, M. R. N.; Sigignono, A.; Tanaka, N.; Musick, W. D. L.; Rossman, M. G. *Proc. Natl. Acad. Sci. U.S.A.* **1981**, *78*, 4767–4771.
(8) Pulsinelli, P. D.; Perutz, M. F.; Nagel, R. L. *Proc. Natl. Acad. Sci. U.S.A.* **1973**, *70*, 3870–3874.
(9) Gerald, P. S.; Ejron, M. L. *Proc. Natl. Acad. Sci. U.S.A.* **1961**, *47*, 1758–1764.
(10) Peisach, J.; Gersonde, K. *Biochemistry* **1977**, *16*, 2539–2545.
(11) Ainscough, E. W.; Addison, A. W.; Dolphin, D.; James, B. R. *J. Am. Chem. Soc.* **1978**, *100*, 7585–7591.
(12) Tang, S. C.; Koch, S.; Papaefthymiou, G. C.; Foner, S.; Fraukel, R. B.; Ibers, J. A.; Holm, R. H. *J. Am. Chem. Soc.* **1976**, *98*, 2414–2433.
(13) (a) Otsuka, T.; Ohya, T.; Satō, M. *Inorg. Chem.* **1984**, *23*, 1777–1779. (b) Otsuka, T.; Ohya, T.; Sato, M. *Inorg. Chem.* **1985**, *24*, 776–782.
(14) Quinn, R.; Nappa, M.; Valentine, J. S. *J. Am. Chem. Soc.* **1982**, *104*, 2588–2595.
(15) Chang, C. K.; Traylor, T. G. *Proc. Natl. Acad. Sci. U.S.A.* **1973**, *70*, 2647–2650.
(16) Momenteau, M.; Rougée, M.; Loock, B. *Eur. J. Biochem.* **1976**, *71*, 63–76.
(17) Momenteau, M.; Loock, B.; Bisagni, E.; Rougée, M. *Can. J. Chem.* **1979**, *57*, 1804–1813.
(18) Collman, J. P.; Braumau, J. L.; Doxsee, K. M.; Halbert, T. R.; Bunneberg, E.; Linder, R. E.; La Mar, G. N.; Del Gaudio, J.; Lang, G.; Spartalian, K. *J. Am. Chem. Soc.* **1980**, *102*, 4182–4192.
(19) (a) Part 2: Momenteau, M.; Mispelter, J.; Loock, B.; Lhoste, J. M. *J. Chem. Soc., Perkin Trans. 1* **1985**, *61*–70. (b) Part 3: Momenteau, M.; Mispelter, J.; Loock, B.; Lhoste, J. M. *J. Chem. Soc., Perkin Trans. 1* **1985**, 221–231.
(20) Lavalette, D.; Tetreau, C.; Mispelter, J.; Momenteau, M.; Lhoste, J. M. *Eur. J. Biochem.* **1985**, *145*, 555–565.

0020-1669/86/1325-4577$01.50/0

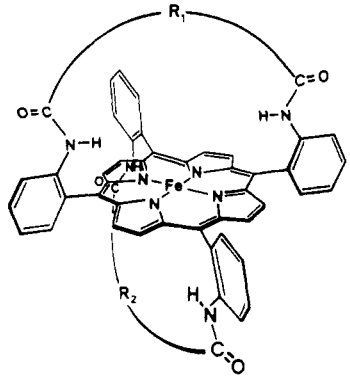

	R_1	R_2
11	$-(CH_2)_{10}-$	$-(CH_2)_4-CHOH-(CH_2)_4-$
12	$-(CH_2)_2-C_6H_4-(CH_2)_2-$	$-(CH_2)_4-CHO^{\ominus}-(CH_2)_4-$
13	$-(CH_2)_4-CHOH-(CH_2)_4-$	$-(CH_2)_4-CHOH-(CH_2)_4-$
14	$-(CH_2)_2-Pyr-(CH_2)_2-$	$-(CH_2)_4-CHOH-(CH_2)_4-$
15	$-(CH_2)_{10}-$	$-(CH_2)_2-Pyr-(CH_2)_2-$
16	$-(CH_2)_{10}-$	$-(CH_2)_4-CH(Im)-(CH_2)_4-$
17	$-(CH_2)_4-CH(Im)-(CH_2)_4-$	$-(CH_2)_4-CH(Im)-(CH_2)_4-$
18	$-(CH_2)_2-C_6H_4-(CH_2)_2-$	$-(CH_2)_2-C_6H_4-(CH_2)_2-$
19	$-(CH_2)_{10}-$	$-(CH_2)_{10}-$
20	$-(CH_2)_7-$	$-(CH_2)_7-$
21	$-(CH_2-$	$-CH_2)_6-$

Figure 1. Amide "basket-handle" porphyrins.

involve two chains each being linked through amide groups to the ortho positions of two opposite phenyl groups of 5,10,15,20-tetraphenylporphyrin (TPP) in a cross-trans configuration.[21]

High-Spin Complexes Fe^{III}–O^-. Intramolecular five-coordination of the ferric ion by the hydroxyl group covalently bonded to one of the two facial chains might be expected for bridged complexes of the type (a-BHP(X)$(CH_2)_4$*CHOH*$(CH_2)_4$)$Fe^{III}Cl$, where X = $(CH_2)_{10}$, $(CH_2)_2C_6H_4(CH_2)_2$, $(CH_2)_4CHOH(CH_2)_4$, and $(CH_2)_2(py)(CH_2)_2$. In fact, their chloroiron(III) complexes (**11**)Cl, (**13**)Cl, and (**14**)Cl exhibit ESR spectra (Figure 2a) typical of high-spin axial species, suggesting no interaction of the alcohol group with the iron ion. In contrast, addition of tributylamine (TBA) to the solution, which is a noncoordinating base (in $CHCl_3$, compounds (TPP)$Fe^{III}Cl$ and (**19**)Cl give a high-spin axial species, even after addition of excess of TBA), leads to ESR spectra typical of high-spin ferric heme with a large rhombic character (Figure 2b) (g = 7.3, 4.5, and 1.79). The rhombic splitting is however larger than that observed for iron(III) protoporphyrin IX di-*tert*-butyl ester and iron(III) protoporphyrin IX dimethyl ester pentacoordinated by RO^-(OEt; OAc) or $PheO^-$(OC_6H_4-4-NO_2; OC_6H_3-3,4-Me_2)[11,12,14] anions. In addition, **12**, which elutes from thin-layer chromatography without any exogenous counterion, exhibits directly the same type of ESR spectrum (Figure 2c) with g values at 7.27, 4.50, and 1.85.

Reactions of the chloroiron(III) complexes (**11**)Cl, (**13**)Cl, and (**14**)Cl with TBA were followed by UV and visible absorption spectroscopy. The electronic absorption spectrum of the chloroiron(III) complex (**11**)Cl in CH_2Cl_2 is illustrated in Figure 3. It is identical with those obtained with chloroiron(III) flat-open porphyrins or with hindered compounds bearing pure alkylene or arylene chains (for example (**19**)Cl). Addition of nitrogenous bases results in nearly identical UV–visible spectral changes. For example stepwise addition of tributylamine (10^{-1} M) to (**11**)Cl (10^{-4} M) results in the formation of a green compound characterized by its visible spectrum with absorption maxima at 418 (ϵ = 92.7 mM), 572 (ϵ = 10.2 mM), and 611 (ϵ = 3.7 mM) nm. This is identical with that of the hydroxoiron(III) derivative,[22] except for a shift of the main visible band of about 10 nm to lower wavelengths. The presence of isobestic points at 500, 536, and

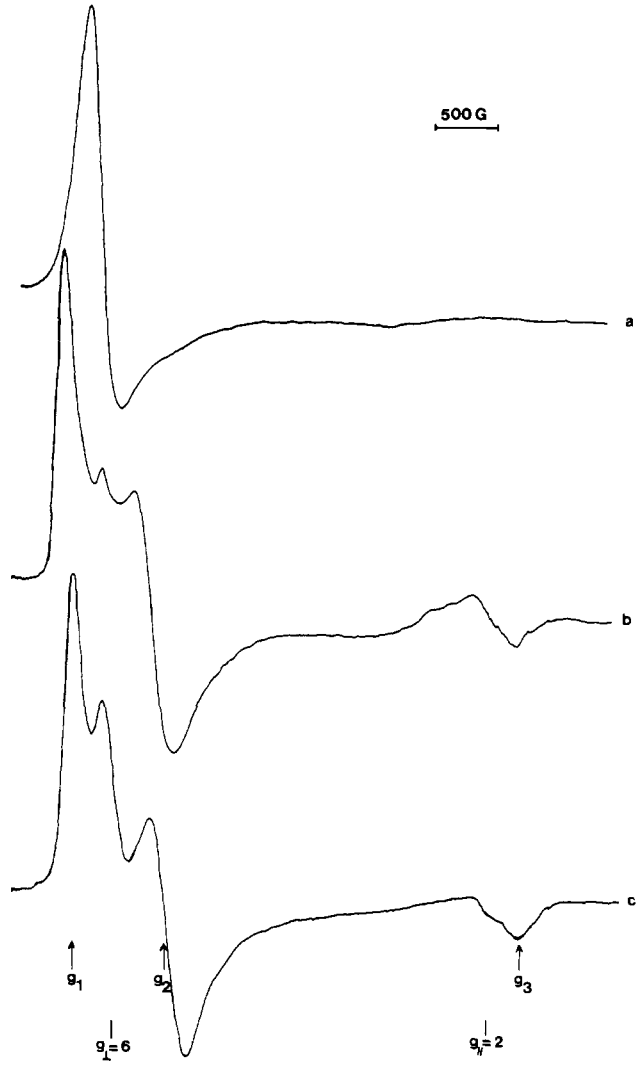

Figure 2. ESR spectra of (a) (**11**)Cl, (b) (**11**)Cl + TBA, and (c) (**12**). In the presence of a rhombic distortion the absorption at g = 6 split into two components g_1 and g_2 while the component at g = 2 shifts to higher field, g_3; see ref 28a.

(21) (a) Momenteau, M.; Loock, B.; Mispelter, J.; Bisagni, E. *Nouv. J. Chim.* **1979**, *3*, 77–79. (b) Part 1: Momenteau, M.; Mispelter, J.; Loock, B.; Bisagni, E. *J. Chem. Soc., Perkin Trans. 1* **1983**, 189–196.

(22) Walker, F. A.; Lo, M.; Ree, M. T. *J. Am. Chem. Soc.* **1976**, *98*, 5552–5560.

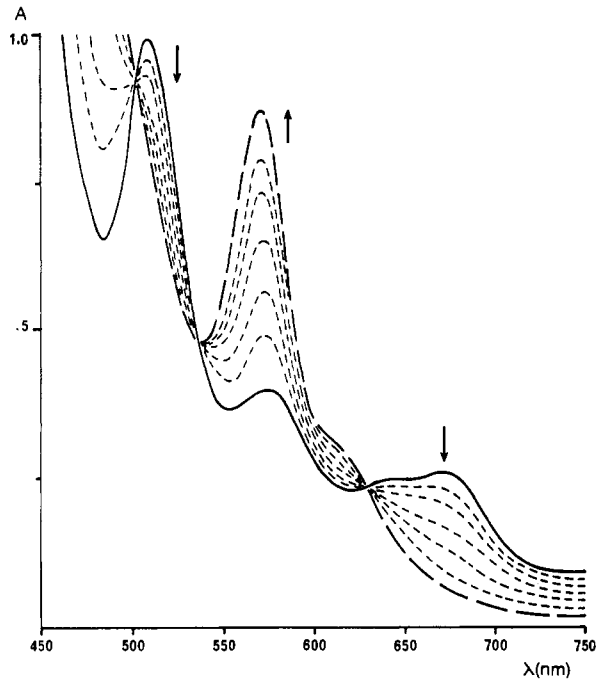

Figure 3. Visible spectral changes upon addition of TBA (10^{-1} M) to a 5×10^{-4} M CH_2Cl_2 solution of (**11**)Cl. Initial spectrum (—), intermediate spectrum (--), final spectrum (– –). The arrows show the increase and the decrease of the bands during the titration.

624 nm indicates that only two absorbing species are present in solution. On the other hand we never observed at room temperature the formation of hemichrome with strong field ligands, such as 1MeIm, in contrast to what is observed during the titration of simple basket-handle porphyrins bearing identical alkylene chains.

Thus, the changes accompanying base addition are indicative of an intramolecular interaction of the type Fe^{III}–O^-, which can be summarized as follows:

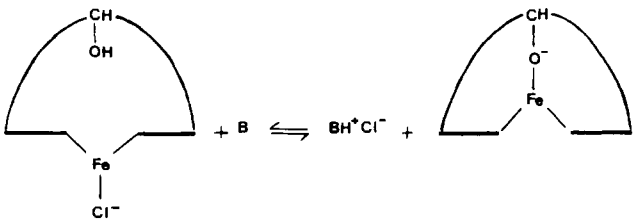

Accordingly, the addition of base to the hemin solution of (**11**)Cl results in the preferential deprotonation of the alcohol group and is followed by the decoordination of the chloride ion, resulting in the formation of a new complex in which the oxyalkylene chain binds to the ferric atom as an iron(III) alkoxide.

Then, compound **12** is identified from its visible spectrum (417, 571, and 611 (sh) nm) and ESR spectrum as the intramolecular liganded complex. In that case, the alkoxo group plays the role of counterion.

Low-Spin Complexes. 1. Axial Ligation Mode O–Fe–O. The five-coordinated complexes described above as Fe^{III}–O^- react with anionic donors (MeO^-, $(Me)_3CO^-$, ...) added in solution to form six-coordinated complexes. This should permit the characterization of the spin state of Fe^{III} in the expected O–Fe–O species, which has been reported to be either in the high-spin[23] or recently low-spin state,[13] depending upon the ligand field strength of the O donors.

In the presence of 1 equiv of MeO^- in solution, the high-spin rhombic ESR spectrum of compound **12** and those of (**11**)Cl and (**14**)Cl treated by TBA converts entirely in a typical low-spin spectrum with g values of 2.42, 2.16, and 1.92, suggesting the formation of a O–Fe–O complex. These g values are indeed close to the first low-spin complex of this type obtained by Sato et al. for Fe (TPP)$(OMe)_2^-$[13] (group C in Table II). Thus it is clear that in these compounds the sixth position is occupied by a MeO^- anion while the alkoxo group of the bridge remains coordinated to the fifth position.

Moreover, we observe that addition of 1 equiv of MeO^- to a solution of compound (**11**)Cl gives a high-spin rhombic complex Fe^{III}–O^-, similar to those described above, which converts also to a low-spin species in the presence of TBA, allowing the ionization of the handle's alcohol group. The corresponding g values (2.48, 2.16, 1.90) are very close to those obtained from compound **12**, also in agreement with an O–Fe–O coordination.

Compound (**13**)Cl, including one alcohol group on each chain, remains unexpectedly a high-spin rhombic Fe^{III}–O^- species even in an excess of TBA. But addition of 1 equiv of RO^- in solution generates a low-spin rhombic species with g values at 2.45, 2.15, and 1.92, characteristic of the axial ligation mode O–Fe–O (see Figure 4a).

2. Axial Ligation Mode O–Fe–N. In this case, our attention was drawn to the possibility of an intrinsic six coordination of the ferric ion from a model with a pyridine group inserted in one chain and an alcohol group covalently attached in the other. As described above, the ESR spectrum of this complex ((**14**)Cl) obtained in $CHCl_3$ after addition of TBA shows a high-spin rhombic species with $g_1 = 7.4$, $g_2 = 4.46$, and $g_3 = 1.80$ assigned to five coordination of the ferric ion by the alkoxo group while one could expect the formation of a six-coordinated species. This suggests that the pyridine inserted in the other handle has a very weak attraction for the metallic ion and that the sixth position remains vacant. Addition of free MeO^- to this solution leads however to the formation of two low-spin species. The first one has been described above as the O–Fe–O type, involving the alkoxo group and MeO^-. The second one (g = 2.65, 2.20, and 1.83) is similar to a low-spin species obtained without ionization of the alcohol group. This latter set of g values suggests that a O–Fe–N axial ligation mode is obtained, involving the endogenous pyridine group and an exogenous MeO^- anion.

Further supports for the characterization of the asymmetric coordination mode O–Fe–N for this type of compounds come from analysis of the (**15**)X and (**16**)X complexes with X^- = Cl^- or OH^-. For X^- = Cl^-, these two compounds show a high-spin axial species, which converts to low-spin when MeO^- is added in solution, while the same low-spin species are directly obtained for X^- = OH^-. The corresponding g values (2.64, 2.19, and 1.83) are in agreement with the axial ligation mode O–Fe–N reported for the Fe(PPIXDBE)(OAr)(py) complex.[11,12] In our case the ferric ion is six-coordinated by the nitrogen atom of imidazole or pyridine group of the chain in the fifth position and by the counterion OH^- or the methoxo anion MeO^- in the other ligation site.

A slightly different low-spin rhombic species is generated from compound (**11**)Cl after addition of TBA and 1 equiv of 1-

Table I. EPR Data for Representative High-Spin Fe^{III}–O^- Complexes

species[a]	g values (77 K)	R,[b] %	ref
12	7.27, 4.51, 1.87	17.2	*c*
(**11**)Cl + TBA	7.34, 4,57, 1.81	17.3	*c*
(**13**)Cl + TBA	7.35, 4.60, 1.91	17.2	*c*
Hb M Boston	6.30, 5.71		8
Fe(OEP)OMe	6.00, 1.9		12
Fe(PPIXDMe)OEt	6.50, 5.50, 1.9	6.2	12
Fe(PPIXDMe)OAc	5.90, 2.0		12
Fe(PPIXDBE)OC_6H_4-4-NO_2	6.2, 2.0		11
Fe(PPIXDBE)OC_6H_3-2,6-$(OMe)_2$	7.90, 5.12, 2.06	17.3	11
Fe(PPIXDBE)OC_6H_3-3,5-$(OMe)_2$	7.20, 5.17, 2.00	12.7	11
Fe(PPIXDBE)OAc	7.83, 5.28, 2.00	15.9	11

[a] Key: Hb, hemoglobin; OEP, octaethylporphyrin; PPIXDME, protoporphyrin IX dimethyl ester; PPIXDBE, protoporphyrin IX di-*tert*-butyl ester. [b] Defined as $(\Delta g/16) \times 100$ where $\Delta g(=g_2 - g_1$—Figure 2b,c) is the absolute difference in g values between the two components near $g = 6$. See ref 28a. [c] This work.

(23) Mashiko, T.; Kastner, M. E.; Spartalian, K.; Scheidt, W. R.; Reed, C. A. *J. Am. Chem. Soc.* **1978**, *100*, 6354–6362.

Table II. EPR Data for Low-Spin Ferric Porphyrin Complexes

label[f]	species	EPR *g* values	tetragonality[a]	rhombicity[a]	ref
		Group C: O–Fe–O			
a	**12** + MeO^- [b]	2.45, 2.16, 1.92	8.537	0.530	*d*
b	(**13**)Cl + TBA + MeO^- [b]	2.45, 2.15, 1.92	8.832	0.506	*d*
c	(**11**)Cl + TBA + MeO^- [b]	2.48, 2.16, 1.90	7.881	0.524	*d*
d	(**20**)Cl + MeO^- [c]	2.44, 2.15, 1.91	8.314	0.542	*d*
e	(**21**)Cl + MeO^- [c]	2.44, 2.15, 1.90	7.976	0.551	*d*
f	(**18**)Cl + MeO^- [c]	2.46, 2.16, 1.91	8.867	0.507	*d*
g	$(TPP)Fe^{III}Cl$ + MeO^- [c]	2.49, 2.16, 1.91	8.850	0.501	13
h	Fe(PPIXDME)(OEt)(py)	2.44, 2.14, 1.92	9.24	0.491	12
i	Fe(OEP)(OCH_3)(1MeIM)	2.43, 2.15, 1.92	8.67	0.535	12
		Group B: O–Fe–N			
j	(**14**)Cl + MeO^-	2.65, 2.21, 1.83	5.587	0.558	*d*
k	(**15**)Cl + MeO^-	2.66, 2.19, 1.83	6.258	0.482	*d*
l	(**15**)OH	2.62, 2.18, 1.86	6.947	0.482	*d*
m	(**16**)OH	2.66, 2.20, 1.83	6.052	0.500	*d*
n	(**16**)Cl + MeO^-	2.68, 2.20, 1.80	5.634	0.509	*d*
o	(**11**)Cl + TBA + 1MeIm	2.50, 2.18, 1.88	6.897	0.552	*d*
p	(**11**)OH + 1MeIm	2.53, 2.17, 1.88	7.255	0.515	*d*
	12 + 1MeIm	high spin[e]			
q	(**19**)OH + 1MeIm	2.57, 2.20, 1.89	6.871	0.528	*d*
r	Fe(PPIXDBE)(OAr)(1MeIm)	2.56, 2.21, 1.85	5.75	0.609	11
s	Fe(PPIXDBE)(OAr)(py)	2.61, 2.19, 1.84	6.23	0.518	11
t	Fe(PPIXDBE)(OAc)(py)	2.61, 2.19, 1.84	6.23	0.518	11
u	Fe^{III}MbOH	2.55, 2.17, 1.85	6.61	0.528	24
		Group A: N–Fe–N			
v	(**17**)Cl	2.89, 2.30, 1.48	2.851	0.672	*d*
w	(**16**)Cl + 1MeIm[b]	2.87, 2.28, 1.55	3.213	0.635	*d*
x	(**19**)Cl + 1MeIm[c]	2.89, 2.30, 1.57	3.239	0.631	*d*
y	$TPP(1MeIm)_2$	2.93, 2.27, 1.53	3.296	0.581	26b
z	*cis*-$((ImCH_2CH_2OCONH_2)_2TPP)Fe^{III}Cl$	2.86, 2.31, 1.55	3.01	0.68	27

[a] The tetragonality (T) and the rhombicity (R) were calculated[31,32] by using a proper axis system.[33] [b] Addition of 1 equiv ($\simeq 5 \times 10^{-3}$ M) in solution. [c] Addition of 2 equiv ($\simeq 10^{-2}$ M) in solution. [d] This work. [e] Due to the steric hindrance of the bridged phenyl group, the space between the bridge and the porphyrin cannot accommodate a 1MeIm molecule. Thus a low-spin complex cannot be formed. [f] The labels refer to Figure 5.

methylimidazole (1MeIm) to the solution. The set of *g* values near 2.5, 2.18, and 1.89, which is close to those reported by Peisach and Mims[24] for ferric MbOH (2.55, 2.17, 1.85), suggests that the imidazole base added in solution is coordinated to the ferric ion, the sixth position being occupied by the alkoxo group of the chain. Likewise, because of the possibility of the counterion OH^- acting as a ligand for Fe^{III}, revealed from ESR data of compounds (**15**)OH and (**16**)OH, we analyzed the behavior of compound (**11**)OH in the presence of 1MeIm without addition of TBA. Under these conditions, the complex gives a low-spin species with *g* values (2.52, 2.18, 1.88) close to those of **15** and **16** (Figure 4c). It seems reasonable to assume that, in this case, the oxygen anionic donor of the intramolecular coordination is substituted by the counterion OH^-.

3. Axial Ligation Mode N–Fe–N. A typical EPR spectrum is shown in Figure 4b. The bis(ligand) complex of compounds (**19**)Cl and (**20**)Cl obtained with 1-methylimidazole in frozen solution give ESR signals at or near 2.92, 2.3, and 1.53, which are characteristic of the axial ligation mode N–Fe–N already described and reported for natural[25] and synthetic[14,26,27] hemin complexes. But compound (**17**)Cl, which includes in both handles an imidazole ring, exhibits without any excess of bases added in solution a low-spin rhombic species with *g* values at 2.89, 2.30, and 1.48, entirely consistent with the axial ligation mode N–Fe–N reported above. We therefore formulate this species as the first well-defined intramolecular N–Fe–N six coordination of the ferric ion in synthetic compounds (Figure 4d).

Discussion

The first intramolecular five coordination of Fe^{III} involving a Fe^{III}–O^- bond in synthetic porphyrin complexes was obtained either directly (**12**) or by ionization of the alcohol group of complexes (**11**)Cl, (**13**)Cl, and (**14**)Cl. This coordination mode leads to characteristic high-spin rhombic ESR spectra with a ratio of the spin-Hamiltonian parameter E/D equal to 0.07, corresponding to about 17% rhombicity.[28a] This rhombic splitting is the largest as compared to that for all other structurally unconstrained flat open iron(III) porphyrin models[12,14] and may reflect contrainst imposed by the chain carrying the alkoxo group, a mechanism which was already proposed by Peisach and co-workers[29] for the explanation of deviations from tetragonal symmetry in hemoproteins.

These pentacoordinated models are also well-defined starting compounds for the analysis of the properties of six-coordination modes like O–Fe–O and O–Fe–N. They could be obtained by addition of the sixth ligand in solution but never when it was incorporated in the second bridge of the basket-handle porphyrins. The reason is probably the constraint and affinity of this potential sixth ligand. As a matter of fact, iron in compound (**14**)Cl is preferentially coordinated by the alkoxo group rather than by the pyridine molecule in agreement with a lower affinity for this base than for O^- anion. But, a subtle balance between steric effect and affinity is suggested by the fact that if free MeO^- anion is added to the solution, a low-spin O–Fe–N species is generated,

(24) Peisach, J.; Mims, W. B. *Biochemistry* **1977**, *16*, 2795–2799.
(25) (a) Watari, H.; Grandinsky, O.; Labeyrie, F. *Biochem. Biophys. Acta* **1967**, *131*, 592–594. (b) Schleyer, H. *Ann. N. Y. Acad. Sci.* **1973**, *212*, 57–73.
(26) (a) Momenteau, M. *Biochem. Biophys. Acta* **1973**, *304*, 814–827. (b) Momenteau, M.; Mispelter, J.; Lexa, D. *Biochem. Biophys. Acta* **1973**, *320*, 652–662.
(27) Walker, F. A.; Reis, D.; Balke, V. L. *J. Am. Chem. Soc.* **1984**, *106*, 6888–6898.
(28) (a) Peisach, J.; Blumberg, W. E. *Probes of Structure and Function of Macromolecules and Membrane*; Chance, B., Yonetani, T., Midvan, A., Eds.; Academic: New York, 1970; Vol. II, p 231. (b) Blumberg, W. E.; Peisach, J. *Probes of Structure and Function of Macromolecules and Membrane*; Chance, B., Yonetani, T., Mildvan, A., Eds.; Academic: New York, 1970; Vol. II, p 215.
(29) (a) Peisach, J.; Appleby, C. A.; Blumberg, W. E. *Arch. Biochem. Biophys.* **1972**, *150*, 725–732. (b) Peisach, J.; Blumberg, W. E.; Ogawa, S.; Rachmilewitz, E. A.; Oltzik, R. *J. Biol. Chem.* **1971**, *246*, 3342–3345.

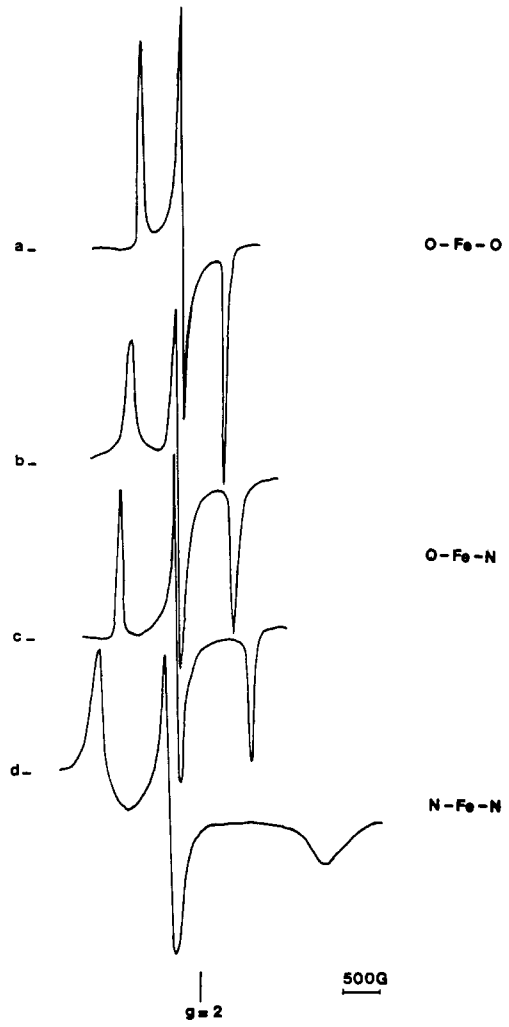

Figure 4. Characteristic spectra of (a) the O–Fe–O axial ligation mode (obtained from (**11**)Cl + TBA + MeO^-), (b + c) the O–Fe–N mode (obtained from (**15**)Cl + MeO^- (b) and obtained from (**11**)OH + 1MeIM (c)), and (d) the N–Fe–N axial ligation mode (obtained from (**16**)Cl + 1MeIm).

suggesting the coordination of pyridine and replacement of the alkoxo group by MeO^-. Moreover, the second alkoxo group of compound (**13**)Cl never binds to iron as well. In that case, the most probable reason is that iron out-of-plane displacement[30] toward the first coordinated alkoxo group renders difficult the approach of the second group, which is hindered by its covalent binding to the bridging chain.

Nevertheless, all of the six-coordinated iron complexes of this study could be obtained with at least one intramolecular ligand. Three notable exceptions can be however distinguished. As far as the counterion OH^- could be considered as intramolecular, compound (**15**)OH and (**16**)OH exhibit low-spin ESR spectra assigned to the group O–Fe–N. It should be however noted that a high-spin species remains in a larger proportion ($\simeq$10%) for (**15**)OH than for (**16**)OH. This is in agreement with a greater affinity of the ferric ion for imidazole (**16**) than for pyridine (**15**). A similar relationship was observed when these bases are exogenous.[22] The third exception is compound (**17**)Cl, which includes an imidazole ring in each handle. This model exhibits indeed a well-defined intramolecular six coordination as revealed by its ESR spectrum. In contrast, compound *cis*- or *trans*-$((ImCH_2CH_2OCONH_2)_2TPP)Fe^{III}Cl$ was reported by Walker and co-workers[27] as a mixture of high-spin (Fe^{III}–N) and low-spin (N–Fe–N) species due to the possibility of inter- and intramolecular coordination to Fe^{III}.

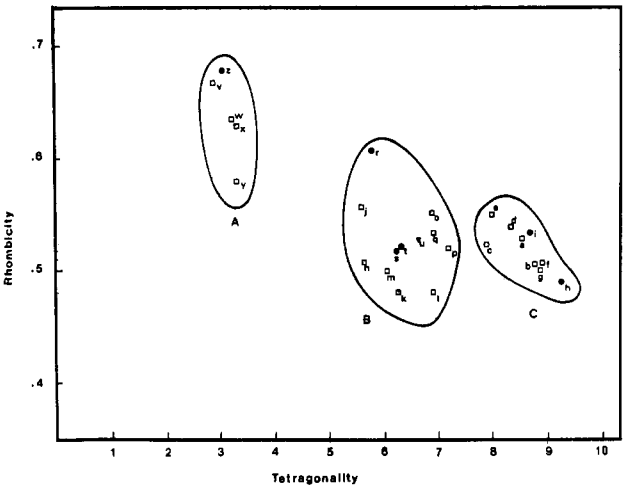

Figure 5. Plot of rhombicity vs. tetragonality for representative complexes: (□) this work; (●) obtained from other porphyrin complexes; (▼) MbOH, see ref 28b. Labels are given in table II.

The low-spin complexes obtained as described above can be classified according to their g values into three distinct groups (Table II), allowing identification of the nature of the axial ligands. For comparison data for some relevant porphyrin complexes of the literature[11-13,26,27] are also given in Table II. A perhaps more clear presentation of the results is depicted in Figure 5 on a Blumberg–Peisach crystal field diagram.[28b] The usual crystal field parameters, i.e. the tetragonality T (Δ/λ) and rhombicity R (v/Δ), were calculated from the observed g values as described by Bohan[31] and Taylor.[32] Among the three possibilities satisfying certain relationships between the g values,[31,32] we kept that giving $R < {}^2/_3$. Although this restriction may be debatable, the diagram provides a clear distinction between the three groups of low-spin complexes assigned respectively to N–Fe–N (group A), O–Fe–N (group B), and O–Fe–O (group C) axial modes of coordination. In addition, the trend among these three groups in the tetragonality, which represents the ligand field strength, follows qualitatively the electronegativity of the axial ligands as expected.

Within this description, keeping in mind that the crystal field parameters derived here should be considered with caution in absence of any knowledge of the relationship between the **g** tensor axis and the heme axis, complexes h and i already assigned to O–Fe–N coordination modes seem in fact to correspond to O–Fe–O type complexes (Table II). The main argument against the previous assignment comes from the observed lower g value of 1.92, which does not fit with that of the O–Fe–N group.

The present study shows that a strict control of the coordination of the ferric ion in porphyrin systems can be realized with the new a-BHP models, and provides new criteria for the characterization of the different type of axial ligation modes of Fe^{III} in hemoproteins. They allow axial coordination by intramolecular ligands such as O^-, pyridine, or imidazole as well as by the counterion OH^-. This removes the often critical assignment of the ligation groups when they were added in excess in unencumbered iron porphyrin solution.

Experimental Section

Physical Measurements. ^1H NMR spectra of free base porphyrins in deuteriochloroform ($CDCl_3$) (CEA, France) were recorded on a Varian XL 100 spectrometer in the Fourier Transform mode using 4K data points in the frequency domain. ESR measurements were carried out on a Varian V-4502 X band spectrometer at 77 K in $CHCl_3$. The magnetic field strength was computed from the nuclear resonance frequency of a proton probe located to the cavity (Varian F 8 A magnetometer). This frequency v was determined with a Hewlett Packard 5245L frequency counter. H is obtained by the relation H (G) =

(30) Hoard, J. L.; Hamor, M. J.; Hamor, T. A.; Caughey, W. S. *J. Am. Chem. Soc.* **1965**, *87*, 2312–2319.

(31) Bohan, T. L. *J. Magn. Reson.* **1977**, *26*, 109–118.

(32) Taylor, C. P. S. *Biochem. Biophys. Acta* **1977**, *491*, 137–149.

(33) Palmer, G. *Iron Porphyrins, Part II*; Lever, A. B. P., Gray, H. B., Eds.; Addison-Wesley: Reading, MA, 1983; p 43.

Scheme I

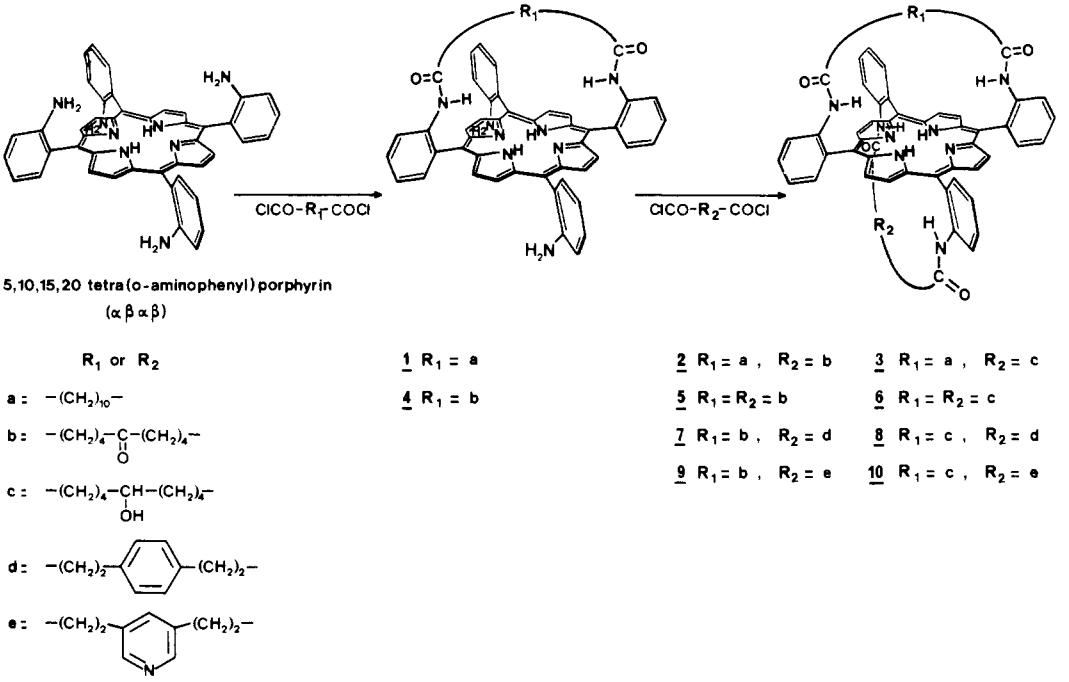

0.234868ν (kHz). The microwave frequency was measured with a calibrated wave meter. The sample concentration was about 5×10^{-3} M. UV–visible spectra were recorded on a Varian DMS 100 in methylene chloride at 25 °C.

Materials. All chemical used were of reagent grade and purchased from Aldrich and Prolabo. Tetrahydrofuran (THF) was purified by distillation from benzophenone–sodium before use. Merck silica gel 60 (60–40 μm) was used for column chromatography. Merck precoated preparative plates (silica gel 60, 2 mm) were used for tlc. Elemental analyses were carried out by the Service Central de Microanalyse du CNRS. Compounds **11–14** were prepared following the procedures described below (Scheme I). Compounds **15–21** were made by published procedures.[21b]

Syntheses. α-5,15-[2,2′-(6-Oxoundecanediamido)diphenyl]-β-10,20-[2,2′-(dodecanediamido)diphenyl]porphyrin (2). This compound was obtained from the single face hindered α-5,15-[2,2′-(dodecanediamido)diphenyl]β-10,20-bis(*o*-aminophenyl)porphyrin (**1**) (1.240 g, 1.43 mmol) and 5-oxononane-1,9-dicarboxylic acid chloride prepared from the corresponding diacid (393 mg, 1.7 mmol), following the previously procedure described for the synthesis of amide-basket-handle porphyrins.[21b] The crude product was purified by column chromatography with a yield of 1.1 g, 72.3%. Anal. Calcd for $C_{67}H_{66}N_8O_5 \cdot 2H_2O$: C, 73.2; H, 6.42; N, 10.19. Found: C, 73.71; H, 6.45; N, 9.70. ^{1}H NMR (ppm): 8.85 (s, 8 × H pyr), 8.64 (d, J = 8 hz, 2 × H_6 Ph), 8.47 (d, J = 8 Hz, 2 × H'_6 Ph), 8.20–7 (m, 12 × H Ph), 6.7 and 6.58 (s, 4 × N*H*CO), 1.52 to −0.44 (18 × methylene), −2.65 (s, 2 × NH).

α-5,15-[2,2′-(6-Hydroxyundecanediamido)diphenyl]-β-10,20-[2,2′-(dodecanediamido)diphenyl]porphyrin (3). To a solution of compound **2** (1.1 g, 1 mmol) in methanol (200 mL) was added 400 mg (10 mmol) of $NaBH_4$. The reaction mixture was stirred at room temperature for 2 h. After addition of water (250 mL) and H_2SO_4 (0.1 M), the solution was extracted with CH_2Cl_2. The organic layer was successively washed with water (×2), aqueous sodium hydrogen carbonate, and water and then dried (Na_2SO_4). The product was crystallized from CH_2Cl_2/hexane. Yield: 1,1 g, 98%. Anal. Calcd for $C_{67}H_{68}N_8O_5 \cdot H_2O$: C, 74.28; H, 6.51; N, 10.34. Found: C, 74.44; H, 6.67; N, 9.98. ^{1}H NMR (ppm): 8.73 (d, 8 × H pyr), 8.54 (m, 4 × N*H*CO), 8.16–7.6 (16, H Ph), 1.55–0.9 (18 × methylene + 1 × C*H*OH), −2.64 (s, 2 × NH + 1 × CHO*H*).

α-5,15-[2,2′-(6-Oxoundecanediamido)diphenyl]-β-10,20-bis(*o*-aminophenyl)porphyrin (4). This compound was prepared by direct coupling of 5,10,15,20-tetrakis(*o*-aminophenyl)porphyrin ($\alpha\beta\alpha\beta$) (1.35 g, 2 mmol) with the diacid chloride of 5-oxononane-1,9-dicarboxylic acid according to the procedure described for amide-basket-handle porphyrins.[21b] Chromatography on a silica gel column gave three major fractions, which were assigned separately by ^{1}H NMR spectroscopy. The first fraction eluted with CH_2Cl_2/ether (10/1) corresponded to the starting material. Yield: 272 mg, 20%. Elution with CH_2Cl_2/acetone (2/1) gave the title compound **4**. Yield: 805 mg, 46.5%. A more polar fraction was obtained by eluting with CH_2Cl_2/acetone (1/1), which was assigned to the symmetric basket-handle α-5,15-β-10,20-bis[2,2′(6-oxoundecanediamido)-diphenyl]porphyrin (**5**). Yield: 443 mg, 21%.

Compound **4**. Anal. Calcd for $C_{55}H_{48}N_8O_3 \cdot 2H_2O$: C, 72.99; H, 5.79; N, 12.38. Found: C, 73.54; H, 5.81; N, 12.32. ^{1}H NMR (ppm): 8.89 (m, 8 × H pyr), 8.34 (d, 2 × H_6 Ph), 8.14–7.08 (m, 12 × H Ph), 6.16 (s, 2 × NHCO), 3.41 (s, 2 × NH_2), 1.41 to −0.25 (m, 8 × methylene), −2.64 (s, 2 × NH).

Compound **5**. Anal. Calcd for $C_{66}H_{62}N_8O_6 \cdot H_2O$: C, 73.31; H, 5.97; N, 10.36. Found: C, 73.31; H, 5.91; N, 10.75. ^{1}H NMR (ppm): 8.85 (s, 8 × H pyr), 8.46 (d, 4 × H_6 Ph), 8.24–7.55 (m, 12 × H Ph), 6.57 (s, 4 × NHCO), 1.38 to −0.18 (16 × methylene), −2.70 (s, 2 × NH).

α-5,15-β-10,20-Bis[2,2′-(6-hydroxyundecanediamido)diphenyl]-porphyrin (6). The procedure described for the preparation of compound **3** was followed. A 400-mg sample of diketone porphyrin **5** was used. **6** was purified by column chromatography using CH_2Cl_2/acetone (1/2) as eluent and was crystallized from CH_2Cl_2/ethanol/hexane. Yield: 345 mg, 86%. Anal. Calcd for $C_{66}H_{66}N_8O_6 \cdot H_2O$: C, 73.04; H, 6.32; N, 10,32. Found: C, 73.04; H, 6.30; N, 10,28. ^{1}H NMR (ppm): 8.90 (m, 8 × H pyr), 8.50–7.54 (m, 16 × H Ph), 6.65 (d, 4 × NHCO), 1.51 to −1.32 (m, 16 × methylene + 2 × C*H*OH), −2.84 (s, 2 × NH), −3.10 (s, 2 × CHO*H*).

α-5,15-[2,2′-(6-Hydroxyundecanediamido)diphenyl]-β-10,20-[2,2′-(3,3′-(*p*-phenylene)dipropionamido)diphenyl]porphyrin (8). **7**, obtained by the coupling reaction of **4** (120 mg, 0.14 mmol) with the diacid chloride of benzene-1,4-bis(propionic acid)[21b] (30 mg, 0.15 mmol) according to the foregoing procedure for the preparation of **2**, was purified by column chromatography with CH_2Cl_2/acetone (5/1). (Yield: 81 mg, 55%.) This was reduced by a reaction analogous to that described above to give the title compound, which was crystallized from CH_2Cl_2/hexane. Yield: 70 mg, 83%. Anal. Calcd for $C_{67}H_{60}N_8O_5 \cdot 3H_2O$: C, 72.41; H, 5.98; N, 10.08. Found: C, 72.73; H, 5.70; N, 10.09. ^{1}H NMR (ppm): 8.90 (d, 8 × H pyr), 8.47 (d, 4 × H_6 Ph), 8.2–7 (m, 12 × H Ph), 6.69 (s, 2 × N*H*CO), 5.78 (d, 2 × *NH*CO), 4.25 (s, 4 × H Ph), 1.54–1.15 (24 × methylene + 1 × C*H*OH), −2.60 (2 × NH + 1 CH*OH*).

α-5,15-[2,2′-(6-Hydroxyundecanediamido)diphenyl]-β-10,20-[2,2′-(pyridine-3,5-diyldipropionamido)diphenyl]porphyrin (10). Coupling reaction of monohandle porphyrin **4** (345 mg, 0.4 mmol) with the diacid chloride of the pyridine derivative[21b] gave the ketone porphyrin **9**. (Yield: 247 mg, 58.8%.) The title compound was then obtained by the usual $NaBH_4$ reduction. Preparative thin-layer chromatography on silica gel plates developed with CH_2Cl_2/acetone (1/1) and subsequent crystallization from CH_2Cl_2/hexane afforded **10**. (Yield: 464 mg, 84%.) Anal. Calcd for $C_{66}H_{59}N_9O_5 \cdot 4H_2O$: C, 70.13; H, 5.97; N, 11.15. Found: C, 70.91; H, 5.78; N, 11.08. ^{1}H NMR (ppm): 8.9 (m, 8 × H pyr), 8.45 (d, 4 × H_6 Ph), 8.25–7.45 (m, 12 × H Ph), 7.6 (m, 2 × H_2 py), 5.7 (s, 2 × N*H*CO), 5.5 (s, 2 × *NH*CO), 3.05 (s, H_4 py), 1.45 and 1.33 (each t, 2 × COCH_2CH_2), 0.4 (s, −C*H*OH), 0.24 (m, 4 × $COCH_2CH_2$), −0.42 (m, CH_2CH_2CH + CH_2(py)), −0.7 (m, CH_2CH_2CH + CH_2CH_2(py)),

–0.95 (m, CH_2CH_2CH), –2.46 (CHOH), –2.5 (s, 2 × NH).

Iron(III) Derivatives (11–14). Iron complexes were synthesized in dimethylformamide by using anhydrous iron(II) chloride and purified as previously described.[21b] Chloroiron(III) and hydroxyiron(III) derivatives were generated by shaking a toluene solution of the metalloporphyrins with aqueous sodium chloride and aqueous sodium carbonate, respectively.

Acknowledgment. This work was supported by the Institut National de la Santé et de la Recherche Médicale.

Contribution from the Department of Chemistry and the Molecular Structure Center, Indiana University, Bloomington, Indiana 47405, and the Department of Chemistry, Manchester University, Manchester M13 9PL, U.K.

Isolation and Structure of $[V(OSiMe_3)(edt)_2]^-$ (edt^{2-} = Ethane-1,2-dithiolate), an Intermediate in the Conversion of $[VO(edt)_2]^{2-}$ to $[VS(edt)_2]^{2-}$ with $(Me_3Si)_2S$. EPR Characterization of the Series $[VE(LL)_2]^{z-}$ (E = O, S, $OSiMe_3$, LL = edt; E = O, LL = pdt)

Joanna K. Money,[1a] Kirsten Folting,[1b] John C. Huffman,[1b] David Collison,[1c] John Temperley,[1c] Frank E. Mabbs,*[1c] and George Christou*[1a]

Received June 12, 1986

The isolation and crystal structure of an intermediate in the conversion of $[VO(edt)_2]^{2-}$ (edt = ethane-1,2-dithiolate) to $[VS(edt)_2]^{2-}$ with $(Me_3Si)_2S$ is reported. $(PPh_4)[V(OSiMe_3)(edt)_2]$ crystallizes in triclinic space group $P\bar{1}$ with a = 12.694 (4) Å, b = 14.901 (5) Å, c = 8.944 (2) Å, α = 96.87 (2)°, β = 94.15 (2)°, γ = 104.30 (2)°, and Z = 2. The anion contains a discrete, five-coordinate, approximately square-pyramidal vanadium(IV) center with V–O = 1.7608 (27) Å, mean V–S = 2.322 Å and mean O–V–S = 107.39°. Fluid and frozen solution EPR spectra on the series $[VE(edt)_2]^{2-}$ (E = O, S, $OSiMe_3$) and on $[VO(pdt)_2]^{2-}$ (pdt = propane-1,3-dithiolate) at X-band frequencies are reported. These data in conjunction with the electronic absorption spectra have been interpreted in terms of a molecular orbital scheme for the antibonding metal d orbitals in the complexes.

Introduction

Recently we reported the preparation, structures and some properties of the vanadium thiolate anions $[VE(edt)_2]^{2-}$ (edt^{2-} = ethane-1,2-dithiolate; E = O (**1**), E = S (**2**)).[2] These species are five-coordinate and square pyramidal with the multiply bonded atom occupying the apical position and four thiolate sulfur atoms occupying the basal positions. Our interest in such species is threefold: (i) to redress the lack of characterized thiolate complexes in the otherwise well-explored area of vanadium(IV) chemistry; (ii) to have at hand vanadium–thiolate species that could act as models for any vanadium–cysteine linkages which might be detected in biological systems; (iii) to investigate the possibility of using mononuclear vanadium thiolates as "building-blocks" for the assembly of higher nuclearity vanadium aggregates. In the latter respect the synthesis of **2** was particularly desirable over **1** in that it contains the highly reactive thiovanadyl (VS^{2+}) unit, allowing the possibility of generating unknown $[V/S/SR]_n$ ($n \geq 2$) species.

Complex **1** was converted to **2** by treatment with hexamethyldisilathiane, $(Me_3Si)_2S$. We herein report the trapping, isolation, and structural characterization of an intermediate in this conversion, $[V(OSiMe_3)(edt)_2]^-$ (**3**). This species provides further progress toward objective i and represents another highly reactive potential "building-block" toward objective iii. In addition, the identification of **3** provides an illuminating insight into the mechanistic pathway from **1** to **2**. We also report the detailed characterization by electron paramagnetic resonance (EPR) spectroscopy of the three-membered series $[VE(edt)_2]^z$ (E = O, S, $OSiMe_3$), a rare opportunity to investigate the effects of varying apical groups in three complexes possessing a basal ligand constancy, and of the related compound $[VO(pdt)_2]^{2-}$ (pdt^{2-} is propane-1,3-dithiolate).

Experimental Section

All manipulations were performed with use of standard inert-atmosphere techniques and a purified dinitrogen atmosphere. Acetonitrile (CaH_2) and diethylether (Na/benzophenone) were distilled and degassed prior to use. $NaSSiMe_3$ was prepared as described elsewhere.[3] Hexamethyldisilathiane (Petrarch) was used as received. $(PPh_4)Na[VO(edt)_2]\cdot 2EtOH$ and $(PPh_4)Na[VS(edt)_2]\cdot xEt_2O$ were available from previous work.[2]

Synthesis of $(PPh_4)[V(OSiMe_3)(edt)_2]$. A slurry of green $(PPh_4)Na[VO(edt)_2]\cdot 2EtOH$ (703 mg, 1 mmol) in MeCN (15 mL) was treated with excess hexamethyldisilathiane (2.0 mL, 9.5 mmol). The green solid rapidly dissolved, and an intense red-purple homogeneous solution was obtained. A large excess of ether (225 mL) was then added as quickly as possible to begin precipitation of a black solid, and the mixture was cooled to –20 °C in a freezer for 1 h. The crude product, contaminated with traces of the thiovanadyl species (**2**), was collected by filtration, washed with ether, and dried in vacuo. The solid was dissolved in room-temperature MeCN (25 mL) and filtered, and ether (175 mL) was added. Overnight storage at –20 °C yielded the analytically pure material as well-formed black prisms in 28% overall yield. Anal. Calcd for $C_{31}H_{37}OPS_4SiV$: C, 56.09; H, 5.62; S, 19.32. Found: C, 56.23; H, 5.81; S, 19.59.

Conversion of $[V(OSiMe_3)(edt)_2]^-$ to $[VS(edt)_2]^{2-}$ with $NaSSiMe_3$. A solution of $(PPh_4)[V(OSiMe_3)(edt)_2]$ (0.081 g, 0.12 mmol) in MeCN (10 mL) was treated with 1 equiv of $NaSSiMe_3$ (0.016 g, 0.12 mmol). The red-purple color slowly changed to orange-brown. After a total of 36 h, ether (15 mL) was added to precipitate a fine brown solid. This was collected by filtration, washed with ether, and dried. Its infrared spectrum was identical with that of authentic $(PPh_4)Na[VS(edt)_2]\cdot xEt_2O$.

Synthesis of $Na_4(acac)_2[VO(pdt)_2]\cdot 2DMF$. A solution of Na_2pdt (45 mmol) in EtOH (100 mL) was prepared from the dithiol (4.52 mL, 45 mmol) and Na metal (2.07 g, 90 mmol). Solid $VO(acac)_2$ (2.98 g, 11.3 mmol) was added with stirring, and as it dissolved a green solution was formed, which rapidly precipitated a light green solid. The solid was collected by filtration, washed with EtOH, and dried in vacuo. Recrystallization from DMF/Et_2O produced long green needles of analytically pure product in 40% overall yield. The presence of monomeric $[VO(pdt)_2]^{2-}$ in this complex salt was confirmed by a crystal structure determination (unpublished work). Anal. Calcd for

(1) (a) Department of Chemistry, Indiana University. (b) Molecular Structure Center, Indiana University. (c) Manchester University.
(2) Money, J. K.; Huffman, J. C.; Christou, G. *Inorg. Chem.* **1984**, *24*, 3297.
(3) Do, Y.; Simhon, E. D.; Holm, R. H. *Inorg. Chem.* **1983**, *22*, 3809.

0020-1669/86/1325-4583$01.50/0